Heliyon 8 (2023) e12608

Contents lists available at ScienceDirect

Heliyon

journal homepage: www.cell.com/heliyon

Research article

Biodiesel synthesized from the blend of *Thai* red and *Elaeis guineensis* oil: An application of calcined base, optimization, kinetics, and thermodynamic parameters studies

U.P. Eyibio [a], K.S. Ukanwa [b], B. Amabogha [c], T.F. Adepoju [c,*], A.D. Adebayo [d], T.A. Balogun [e], A.C. Eloka-Eboka [f]

[a] *Chemical/Petrochemical Engineering Department, Akwa-Ibom State University, Ikot Akpaden Mkpat Enin L.G.A., Akwa-Ibom State, Nigeria, P.M.B 1167, Uyo, Nigeria*
[b] *Centre for Thermal Energy Systems and Materials, School of Water, Energy and Environment, Cranfield University, MK43 0AL, UK*
[c] *Chemical Engineering Department, Federal University Otuoke, Bayelsa State, Nigeria, P.M.B 126, Yenagoa, Nigeria*
[d] *Electrical and Electronic Engineering Department, Federal University, Otuoke, Bayelsa State, Nigeria, P.M.B 126, Yenagoa, Nigeria*
[e] *Chemical Engineering Department, River State University, Port Harcourt, River State, Nigeria*
[f] *Centre of Excellence in Carbon Bases Fuels, School of Chemical and Mineral Engineering, North-West University, Potchefstroom, South Africa*

ARTICLE INFO

Keywords:
Biodiesel
Duhem equation
Mixed oil
Kinetics
Thermodynamics parameters
Littorina littorea shell
Calcined catalyst

ABSTRACT

The study emphasized the use of the mixed oil (MO) extracted from *Elaeis guineensis* and *Thai* Red oilseeds for the synthesis of biodiesel using a derived bio-base catalyst from calcined *Littorina littorea* shell powder. The MO properties were determined with a view to examine its quality for biodiesel production. The derived calcined catalyst was characterized using scanning electron microscopy (SEM), X-ray fluorescence (XRF), Fourier transforms infrared spectroscopy (FTIR), BET adsorption analysis, and Hammett indicator. Process optimization of biodiesel synthesized was carried out by considering four constraint variables: reaction time (60–80 min), catalyst conc. (2–6% wt.), reaction temp.(55–75 °C), and ethanol/oil molar ratio (E-OH/OMR) (4–8 vol./vol.) using design expert STAT EASE 360. For the rate of reaction, degree of disorderliness, and the activation energy of the transesterification process, kinetics and thermodynamic parameters were considered using Eyring Polanyi and Gibb's Duhem equations, while the qualities of biodiesel as well as its economic appraisal were also carried out. Results obtained showed the API gravity ratio of the mixed oil of 2:3, which indicated a perfect blend ratio. Statistical analysis validation via response surface methodology indicated a biodiesel yield of 98.90% (wt./wt.) was obtained at 69.83 (min), 5.86% (wt.), 68.17 °C, and 7.04 (vol./vol.). Kinetic parameter evaluation showed the activation energy (E_a) of transesterification of the mixed oil to biodiesel to be 55.44 kJ mol^{-1} while thermodynamic parameters (Gibb's free-ΔG^{θ}) were obtained as follows: 184.87 kJ mol^{-1}, 179.77 kJ mol^{-1}, and 174.67 kJ mol^{-1}, at enthalpy (ΔH^{θ}) value of 53.38 kJ mol^{-1} and entropy (ΔS^{θ}) of -509.64 J mol^{-1}, respectively. Catalyst reusability test was altered at 7th cycles, while the qualities of biodiesel were found comparable with biodiesel recommended standards (ASTM D6751 and EN 14214).

1. Introduction

Based on Economist Intelligent Unit (EIU) outlook on the growth prospects, top risks, and key trend facing the energy sector in 2022. It has been estimated the Global energy consumption by will rise by 2.2% in 2022 as the economies recover from the impact of the pandemic [1]. It was also proclaimed that by 2040 the world energy consumption will escalate by 77% increase while it has been proven that by 2050, the global energy use for both industrial and domestic could be triple (a rise from 300 to 900 million terajoules) [2]. This is an indication that energy consumption will continue to increase because of geometrical growth in the world population (as far as the number of reproduction rate is higher than the mortality rate). Meanwhile, fossil fuels such as oil, coal, and gas accounted for the 83% of the world energy consumption, but oil is the most sources of energy nationwide [3]. However, the energy supply mix has contributed to global warming (an effects caused by increased levels of carbon dioxide, CFCs, and other pollutant) causing more havoc than any other sources of disasters to human livelihood [4]. Therefore, there is

* Corresponding author.
E-mail addresses: avogadros2002@yahoo.com, avogadros2002@gmail.com, adepojutunde@fuo.edu.ng (T.F. Adepoju).

https://doi.org/10.1016/j.heliyon.2022.e12608
Received 6 August 2022; Received in revised form 7 October 2022; Accepted 16 December 2022

a need to urgently replace the oil with an alternative oils that are renewable, sustainable, readily available, cost effective, and environmentally friendly energy [5].

Renewable energy is on the intensification, but too sluggish [6]. It was anticipated that from 2010 to 2030 the worldwide renewable energy used will rise from 2 to 6% nationwide. Unfortunately, this projected increased in the use of renewable energy oil was not sufficient to cover the global increase in energy demand. Previously, in 2018, the global renewable energy source accounted for 14.5% globally, but this value still accounted for merely a third of the entire intensification [7]. This make the global world to be on an unsustainable pathway along with rising disparity amid collective demands for exploit on environment change and the real pace of growth through energy needs and released of carbon rising at their fastest speed since centuries. One way to rescue the global world from this unsustainable pathway is to harness the oils that can be obtained from waste non-edible seedoil as feedstock for energy production, since the use of conventional oils are the major contributors to the global warming. Therefore, biodiesel synthesis via transterification of non-edible oil as a replacement for diesel oil is the main pathway to sustainable living environment [8].

Biodiesel otherwise known as fatty acid methylester (FAME) is a fuel derived from the reaction between fat/oil and alcohol in the presence of catalyst (NaOH/KOH) to produce an ester and glycerol [9]. Oils have been the major feedstock reportedly used for biodiesel production, but preferable non-edible oils owing to the world food treat vegetable oil claimed [10]. Among non-edible oils whose seeds are available as wastes rich in oil content are *Elaeis guineensis* and *Thai* Red oils. The seeds of the fruit plants have been reportedly used to produced non-edible oils for industrial applications [9, 11]. Catalysts adopted as aids for conversion of oil to biodiesel production (NaOH or KOH) have been reportedly to have some shortcomings such as non-recoverability [12], toxicity, soap formation [9], and high production cost [13]. The used of derived base-catalysts have been established to tackled the above mentioning problems [14] to achieved maximum biodiesel yield. Among the derived base catalysts is the shell of *Littorina littorea* belong to family of snail.

Littorina littorea common name periwinkle is a species of small comestible sea snail; it's marine gastropod mollusca that have gills and an operculum, classified within the family of *Littorina*. The meat is high in protein, omega -3 fatty acids and low in fat [15]. The shells were usually taken with Veneer caliper to remove the meat [16]. However, the shell have been reportedly used in construction of house pillars when mixed with cement, casting material in soak away, filling of pot holes, but high percentage of the shell have been discarded as wastes owing to its relative abundance [17]. Researches showed that the shell powder when calcined at high temperature (>650 °C) have been reportedly used as a bio-base catalyst for biodiesel production [18, 19].

Process modeling and optimization have been established as one way of achieving the optimum product yield during biodiesel synthesis [7, 9] especially when the constraint factors are properly model. Four main factors are key important such as: reaction time for complete production, the reaction temperature for complete conversion, the catalyst concentration required to aid the biodiesel formation, and the alcohol to oil molar ratio required for oil conversion to biodiesel [20].

From overall reports, no single study ever reported the use specific gravity formulation for the blend of oil of *Elaeis guineensis* and *Thai* Red oilseed. Furthermore, no report in the past or present have combined in a single study the kinetic study, thermodynamics parameters, process optimization, and catalyst reusability test in conducting biodiesel synthesis from oil blend, except in this study. Therefore, to cover the research gap and provide literatures for the fourth coming researches, this research utilized the specific gravity ratio formulation for the blend of binary oils, derived bio-based catalyst from calcined *Littorina littorea* shell (periwinkle shell) ash, characterized the calcined ash powder via Scanning Electron Microscopy (SEM), X-ray Fluorescence (XRF), Fourier transforms infrared spectroscopy (FTIR), BET adsorption analysis, and qualitative analysis, carried out the process optimization using design expert 360 Stat Ease with reference to constraint variables (reaction time, reaction temperature, catalyst concentration, and methanol to oil molar ratio), appraise the kinetics and thermodynamic parameters of the transesterification reaction of biodiesel production through Eyring Polanyi and Gibb's Duhem Equations with reference to Arrhenius Equation. Furthermore, the strength of the derived base catalyst was tested after recycled using catalyst reusability test, and biodiesel properties were determined and compared with biodiesel recommended standard with a view to find a sustainable pathway for replacement of conventional diesel and global acceptability.

2. Material and methods

2.1. Materials

Freshly harvested *Elaeis guineensis* seed was collected from Sabo market, the Thai Red seed was obtained from a local palm oil production village, and the *Littorina littorea* shell was acquired from a nearby Market, all are wastes without any cost inquired during the collection. The location is Otuoke, Yenegoa, and Bayelsa State, Nigeria. The seeds and the shell were washed with distilled water, sun-dried for 14 days before the seeds were milled into the powdery form and kept in clean containers for further processing. The *L. littorea* dried shell was calcined at 1000 °C in furnace for 4 h, allowed to cool, and then grinded into powdered form. The grinded powder was sieved into smaller particle powder with 0.3 mm sieve, and was kept in a tight container for further processing.

All chemicals employed in this research work were obtained from laboratory, supplied by Sigma Aldrich and were of standard grades.

2.2. Methods

2.2.1. Extraction of oils

Continuous process was used for oil extraction from the seed powders with N-hexane as solvent. Powder was put in muslin chamber enclosed with condenser as cooling part and a 500 ml round bottom flask was half filled with n-hexane placed on heating mantle for extraction. The extraction temperature was 70 °C maintained for 50–60 min, and the n-hexane in the extracted oil was recycled in an evaporator. The recycled n-hexane was reused for more extractions, and the oils were filtered to obtained pure oils. *Elaeis guineensis* oil is referred to as EGO, while *Thai* Red oil is TRO.

2.2.2. Oil mixed ratio determination

The oil mix ratio was determined using the value of API gravity estimated of each of the oil and total API gravity was obtained by summing up the API gravity of each of the oil. The blending/mixing ratio was then computed by dividing the API gravity of individual oil with the total API gravity. The mixed oil obtained was standardized heating at 100 °C for 20 min in a magnetic shaker. The properties of the oils and the mixed oil were then determined using [9].

2.2.3. Properties of EGO, TRO, and mixed oil (MO)

Properties of the oils were carried out using AOAC, 1997 [21] procedural methods. Major oil requirement properties for biodiesel synthesis were carried out such as: the percentage moisture content; the specific gravity, viscosity, saponification value, iodine value, free fatty acid (FFA), acid value, and peroxide value. Other fuel properties tendencies of the oil such as cetane number, higher heating value, and API gravity were computed as indicated in Eqs. (1), (2), and (3)

Cetane number - (ASTM D2015) [22]

$$CN = 46.3 + \frac{5458}{saponification\ value} - 0.225\ Iodine\ value \quad (1)$$

Higher Heating Value (HHV) - (ASTM D2015) [22].

$$HHV(MJ/kg) = 49.43 - [0.041(Saponification\ value) + 0.015(Iodine\ value)] \quad (2)$$

American Petroleum Institute (API) - Haldar *et al.* (2009) [23].

$$API = \frac{141.5}{SG} - 131.5 \quad (3)$$

2.3. Analysis of calcined L. littorea shell powder (CLLSP)

Analysis of the CLLSP was carried out using the following equipment: SEM to produces a largely magnified image by using electrons instead of light to form an image structure of the CLLSP. The XRS-FP analyser with fundamental parameters (FP) converts elemental peak intensities to elemental concentrations of film thickness for the CLLSP. FTIR analyser to classify the chemical bonds in a molecule by producing an infrared absorption spectrum, the spectra produce a profile of the sample, a distinctive molecular fingerprint that was used to scan the CLLSP to identifies different components. Brunauer-Emmett- Teller (BET) to determine the physical absorption of gas molecule on CLLSP surfaces and measurement of the specific surface area of materials as well as full isotherms for porosity determination [24]. The procedures are as follows.

2.3.1. BET procedure for catalysts analysis

Samples were preheated at temperature above 100 °C for 30 min beneath He-flow to remove some adsorbed overloaded units on the catalyst surfaces, then 0.05 carbon (iv) oxide was entered above the sample with He-gas at flow rate 20 ml/min for 45 min. CO_2-temperature-programmed desorption was used to examined the strength of the samples and the results was reported.

2.3.2. XRF procedure for catalysts analysis

X-ray Fluorescence (XRF) spectrophotometer was used to evaluate the compositional structure of the samples. The XRF was dispersive with a rhodium source at energy disparity of 2.2 kW. The specific surface area of samples was unveiled by BET method using nitrogen desorption isotherm analysis along with volumetric adsorption analyser at 196 °C.

2.3.3. FTIR procedure for catalysts analysis

FTIR spectrometers (Agilent Technologies Model Cary 122 630 FT-IR spectrometer) with spectral range from 400–4000 cm^{-1} rely on the same basic principle as NDIR analyzers. However, FTIR spectroscopy is a disperse method, indicating that the dimensions are done over a wide range instead of a thin ensemble of frequencies. The technique is done by leading an x-ray beam at samples and the intensity of the scattering movement was observed. With the help of the FTIR spectrometer along with IR-beams, the spectra remained assessed and ascertain in line with reference database.

2.3.4. SEM procedure for catalysts analysis

SEM analyser is used to examine the morphology of the powder before merging. The procedure is as follows: A carbon tape with two sides was immobile to SEM sample stub, and the uhmwpe powder is spread on the superficial. The sample was examined in a SEM chamber after the platinum gold light was applied (100 Å). The flakes diameter arranges from 50–100 μm. The surface structures were then observed.

2.4. Transesterification of mixed oil to biodiesel

Since the mixed oil FFA = 0.64% < 1.5% recommended standard for transesterification of oil to biodiesel, Biodiesel production from MO was carried out in a three necked reactor as earlier reported in our work [25] with few modifications. CH_3OH was an alcohol used for process conversion due to its less chemical harmfulness and it ability to possess high activation energy. The process optimization resulted in identification of four key factors affecting biodiesel synthesis were considered using central composite rotatory design (CCRD), an allied of response surface methodology design. The product (biodiesel) formation qualities were ascertained using AOAC (1997), and the properties were compared with biodiesel recommended standard.

Table 1. Design of experimental variables with levels.

Transesterification							
Variables	Units	Symbols	Levels				
			-2	-1	0	+1	+2
Reaction time	(min)	X_1	60	65	70	75	80
Cat. Conc.	(%)	X_2	2	3	4	5	6
Reaction temp.	(^oC)	X_4	55	60	65	70	75
E-OH/oil molar ratio	(vol./vol.)	X_3	4	5	6	7	8

2.5. Experimental design and process optimization of biodiesel synthesis

To design the biodiesel production from the MO, four-factors with five level variables were considered as indicated in Table 1. Design 360 STAT EASE expert version se-13.1.4.0-x64 was used for process optimization, central composite design with polynomial modeling was selected for statistical analysis, and the selected model randomly based on the axes point, central points, and the orthogonality points generated a total of thirty experimental runs, and this was carried out in duplicate and the average means value of biodiesel yield was determined. The algorithm picks points that minimize the integral of the prediction of variance across the design space. The design expert 13.1.4.0 was adopted for this process with four variables; Reaction time: X_1, Cat. Conc.; X_2, Reaction temp: X_3, and E-OH/molar oil ratio: X_4, correspondingly. Other parameter such as stirring speed can also be considered on a large design reactor for the production. In this case, magnetic stirrer was used, and the speed of the stirrer was kept constant at 3500 rpm.

Based on E-OH/oil molar ratio, according to stoichiometric ratio, 1:3 is required for reaction to reach completion, but the yield of biodiesel always low with high waste product (glycerol). Twice ratio (1:6) of methanol-oil molar ratio produce high yield of biodiesel. Hence, the choice of ratio ranges 1:4 to 1:8 selected in the design of variables of this study. Meanwhile, the reaction temperature range were chosen since the

Table 2. Properties of extracted oil comparative.

Properties	*EGO*	TRO	MO	Total API gravity
Density (kg/m^3) @ 30 °C	930.00	874.40	900.20	
Viscosity @ 40 °C/(mm^2/s)	20.50	16.20	18.20	
Moisture content (%)	0.08	0.02	0.06	
%FFA (as oleic acid)	1.15	0.85	0.98	
Acid value (mg KOH/g oil)	2.30	1.70	1.96	
Saponification value (mg KOH/g oil)	240.30	196.30	210.40	
Iodine value (g I_2/100g oil)	15.30	94.50	55.10	
Peroxide value (meq O_2/kg oil)	14.80	5.20	10.00	
HHV (MJ/kg)	39.35	39.96	39.70	
Cetane number	65.57	52.84	59.84	
API gravity	20.65	30.33	25.72	50.98
Heavier/Lighter oil	**Light oil**	**Light oil**	**Light oil**	
Mixed ratio	**40 (2)**	**60 (3)**		

API gravity of oil >10, indicate lighter oil and the oil floats on water, the value of API gravity <10 indicates heavier oil and the oil sinks on water.

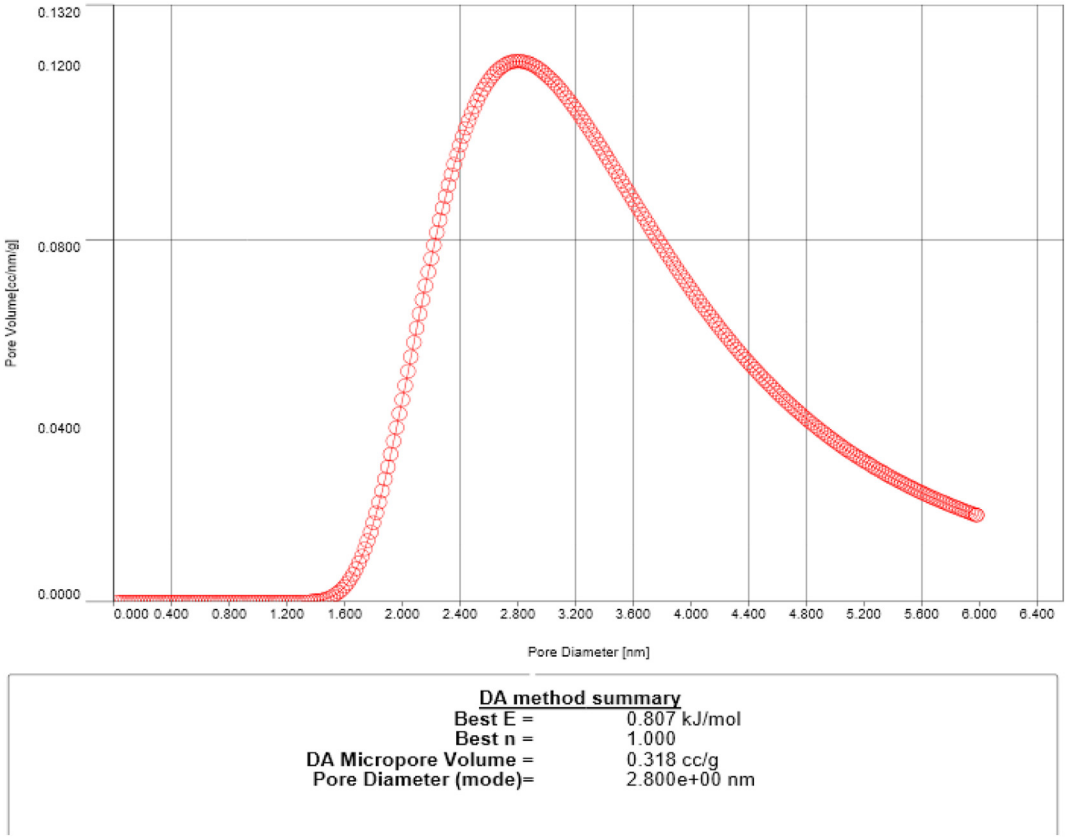

Figure 1. Graph of volume pore vs. diameter pore.

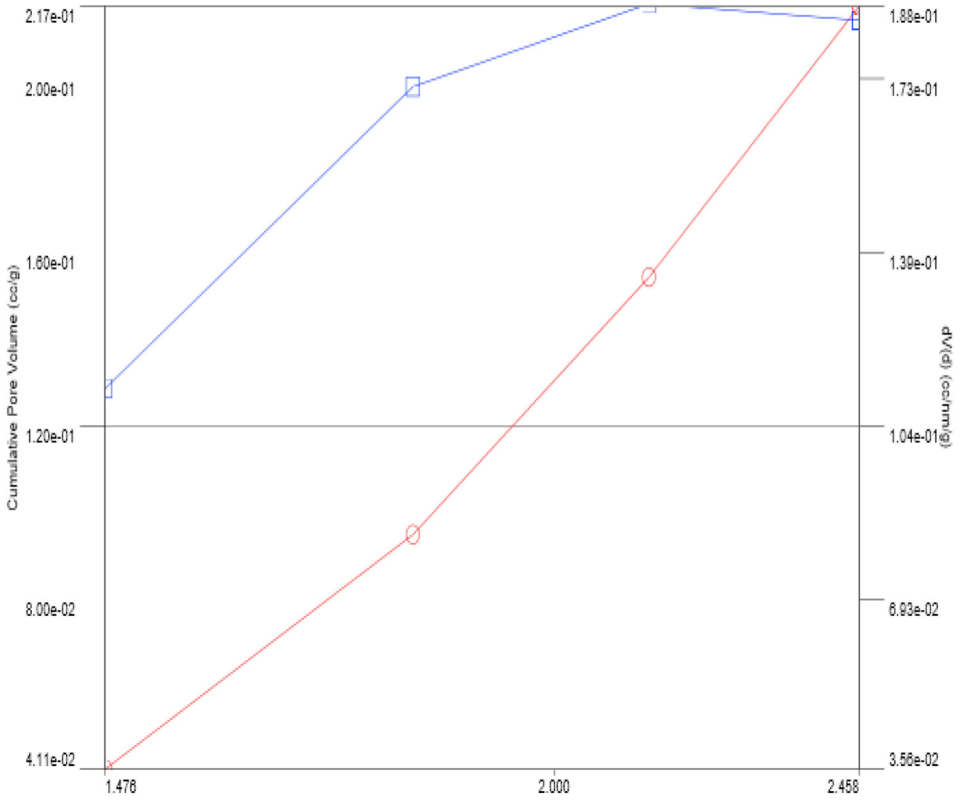

Figure 2. Ternary plot of cumulative pore volume, surface area against pore diameter.

Table 3. XRS-FP analysis report.

Compounds	Concentration (%wt.)	Mole (%)
SiO_2	3.555	3.424
Fe_2O_3	1.704	2.242
CaO	89.457	92.312
MgO	1.142	1.839
Al_2O_3	3.950	2.242
Cl	0.549	0.198
SnO_2	0.549	0.896

boiling point of ethanol is > 70 °C. The choice of lower temperature from 55 to 65 °C was to give room for effects of lower temperature on the yield, but the preheated conditions also favour the biodiesel formation. Temperature >70 °C employed was also to encourage biofuel formation). These ranges have been reportedly employed by some researchers in their published works [7, 26, 27, 28]. Also, since the catalyst major composition was CaO with concentration of 89.457% (wt). A low quantity limits between 2–6% were chosen to aids the formation of biodiesel owing to large surface area with faster rate of reaction. Also, catalyst recoverability is of paramount important, hence the smaller quantities used accounted for recoverability [29, 30, 31]. Meanwhile, a reaction time >60 min have been reportedly enough to convert oil to biodiesel for optimum yield [32, 33, 34, 35].

For process optimization, the variables and the responses of experimental results were statistically analysed step by steps with a view to determine the optimum condition for biodiesel production. Fits statistics test, test of significant, hypothesis test, multiple regression, and analysis of variance were used to test the variables significant, coefficient of determination, and interactive effects amidst the variables in term of the contour and 3-dimensional plots. The polynomial equation that expresses the variation of biodiesel yield with constraint variables is presented in Eq. (4).

$$Y = I + A_1X + A_2X^2 + A_3X^3 + \ldots + A_KX^K \quad (4)$$

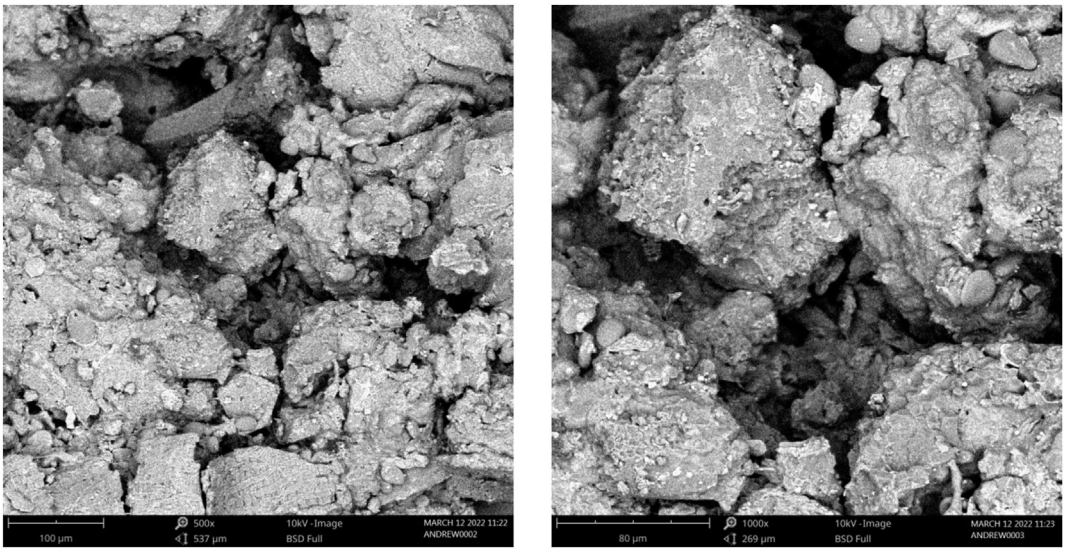

Figure 3. Images of SEM analysis.

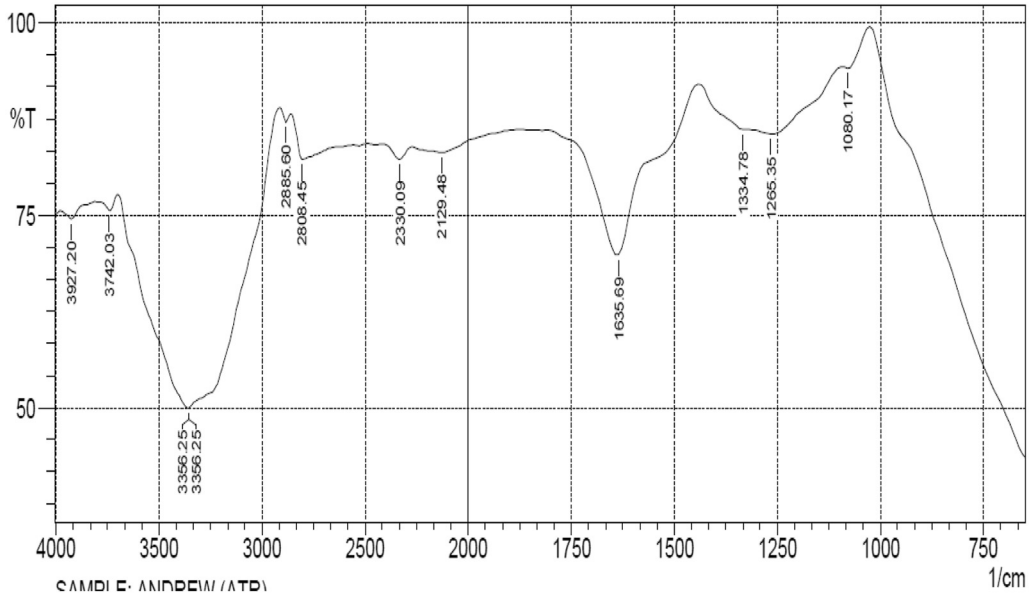

Figure 4. FTIR analysis.

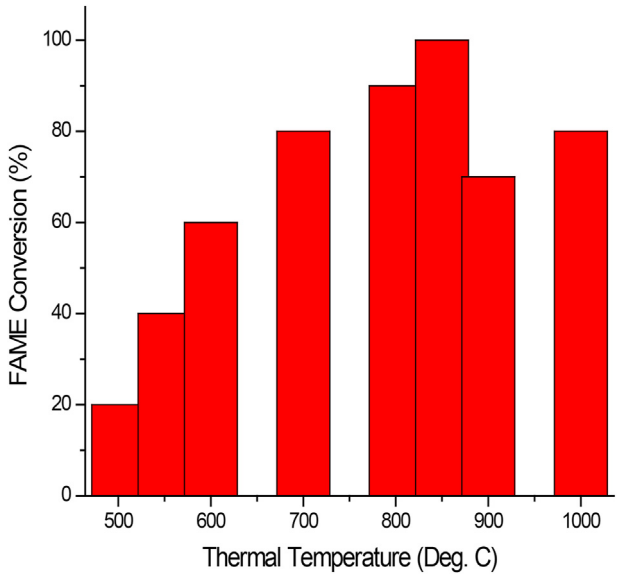

Figure 5. Effects of thermal treatment on catalyst for the conversion of FAME (biodiesel).

Based on the design software the regression parameter were evaluated via the root mean square error (RMSE), coefficient of determination (R^2), adjusted ($R^2_{adj.}$), and predicted ($R^2_{pred.}$), and Eqs. (5), (6), (7), and (8).

$$R^2 = 1 - \frac{SS_{res.}}{SS_{tot}} \tag{5}$$

$$R^2_{adj.} = 1 - \sum_{i=1}^{n} \left(\frac{\in_{i,cal} - \in_{i,\exp}}{\in_{avg,\exp} - \in_{i,\exp}} \right)^2 \tag{6}$$

$$R^2_{pred.} = 1 - \left\{ \frac{\left(1 - R^2_{pred.}\right)(n-1)}{n - (nv+1)} \right\} \tag{7}$$

$$RMSE = \sqrt{\frac{\sum \left(\in_{i,cal} - \in_{i,\exp} \right)}{N}} \tag{8}$$

With $\in_{i,cal}$ computed value, $\in_{i,\exp}$ experimental value, n number of experimental runs, $\in_{avg,\exp}$ average experimental value, nv variables number, $SS_{res.}$ residual sum of square, SS_{tot} total sum of error [36].

2.6. Kinetics of transesterification reaction

Based on transesterification reaction, according to stoichiometric ratio, 1:3 is required between triglyceride and methanol for reaction to reach completion. Therefore, the rate equation can be expressed as in Eq. (9). Since the reaction temperature and time are the major constraint factors in reaction kinetic of transesterification, hence, the model kinetic was performed at optimum parameter of transesterification process with setting temperature at 55, 60, 65, 70, and 75 °C.

Table 4. Experimental biodiesel yield, the predicted yield, the errors, and the variables.

Run	Reaction time (min)	Cat. Conc. (%wt.)	Reaction temp. (deg. C)	E-OH/OMR (vol./vol.)	Biodiesel Yield (% wt./wt.)	Predicted Yield (% wt./wt.)	Error term
1	80	4	65	6	94.22	94.33	-0.1071
2	60	2	75	8	90.73	90.52	0.2092
3	70	4	65	6	98.65	98.67	-0.0167
4	70	4	55	6	90.64	90.76	-0.1171
5	60	2	55	4	90.28	90.25	0.0308
6	*70*	*4*	*65*	*6*	*98.67*	*98.67*	*0.0033*
7	80	6	55	8	95.78	95.83	-0.0538
8	60	6	75	8	93.10	93.22	-0.1238
9	60	6	75	4	93.33	93.16	0.1742
10	80	2	75	8	93.61	93.69	-0.0771
11	80	6	75	4	93.56	93.58	-0.0171
12	60	6	55	8	91.20	91.02	0.1825
13	80	2	55	4	90.00	89.90	0.1046
14	60	4	65	6	90.15	90.30	-0.1521
15	70	8	65	6	96.80	96.94	-0.1388
16	*60*	*2*	*55*	*8*	*86.99*	*86.99*	*-0.0021*
17	80	2	55	8	90.70	90.60	0.1042
18	*70*	*4*	*65*	*6*	*98.67*	*98.67*	*0.0033*
19	60	6	55	4	93.92	93.86	0.0579
20	*70*	*4*	*65*	*6*	*98.67*	*98.67*	*0.0033*
21	60	2	75	4	90.90	90.87	0.0346
22	70	4	75	6	93.00	93.14	-0.1421
23	80	6	55	4	94.79	94.72	0.0692
24	70	2	65	6	89.29	89.41	-0.1204
25	70	4	65	2	91.00	91.15	-0.1454
26	*70*	*4*	*65*	*6*	*98.67*	*98.67*	*0.0033*
27	80	6	75	8	97.85	97.60	0.2475
28	*70*	*4*	*65*	*6*	*98.67*	*98.67*	*0.0033*
29	80	2	75	4	90.17	90.07	0.0958
30	70	4	65	10	91.80	91.91	-0.1138

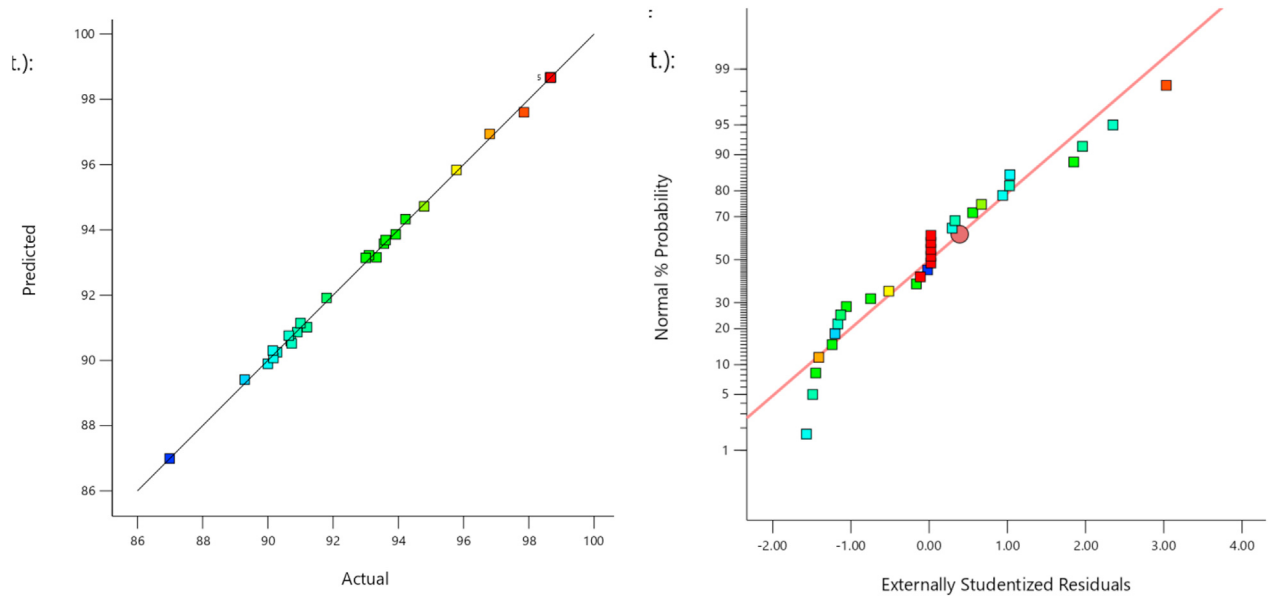

Figure 6. (a). Predicted vs. Experimental (b). Normal prob. vs. Externally SD.

$$Rate(r) = -\frac{d[TG]}{dt} = k[TG][MOH]^3 \quad (9)$$

where r is the rate of reaction (transesterification), k is the rate constant, [TG] is the molar concentration of triglycerides, and [MOH] is the molar concentration of methanol.

To avoid low biodiesel yield and a reversible reaction to take place based on stoichiometric ratio of 1:3 of the transesterification process, stoichiometric ratio, 1:3, a large excess of methanol was added [17], usually twice ratio (1:6) of methanol-oil molar ratio. Hence, the concentration of methanol is assumed a constant value. The reaction can then be a pseudo first order [37].

Rearranging the rate equation and integrate, to obtain Eq. (10):

Table 5. ANOVA test of significance for every regression coefficient.

Source	Sum of squares	df	Mean Square	F-value	P-value
Model	347.52	14	24.82	1003.58	<0.0001
X_1	24.30	1	24.30	982.50	<0.0001
X_2	85.01	1	85.01	3437.13	<0.0001
X_3	8.53	1	8.53	344.97	<0.0001
X_4	0.8855	1	0.8855	35.80	<0.0001
X_1X_2	1.47	1	1.47	59.44	<0.0001
X_1X_3	0.1914	1	0.1914	7.74	0.0140
X_1X_4	15.66	1	15.66	633.21	<0.0001
X_2X_3	1.75	1	1.75	70.71	<0.0001
X_2X_4	0.1702	1	0.1702	6.88	0.0192
X_1^2	8.48	1	8.48	342.96	<0.0001
X_2^2	69.17	1	69.17	2796.55	<0.0001
X_3^2	51.71	1	51.71	2090.57	<0.0001
X_4^2	77.35	1	77.35	3127.18	<0.0001
Residual	87.32	1	87.32	3530.47	<0.0001
Lack of Fit	0.3710	15	0.0247	-	-
Pure Error	0.3707	10	0.0371	556.01	-
Cor. Total	0.0003	5	0.0001	-	-
Fits statistics					
R squared	99.89%				
Adjusted R squared	99.79%				
Predicted R squared	99.39%				

$$-\ln|1 - X_{FAME}| = k.t \quad (10)$$

With k as rate constant measure in min^{-1}, X_{FAME} stands for FAME conversion at interval time (t). From Eq. (10), the graph of $-ln|1 - X_{FAME}|$ vs t was plotted, and the slope of the graph was determined. The slope of the graph represents the rate constant k.

Furthermore, energy must be added to the reactants to overcome the energy barrier, which is recovered when products formation occur. This energy is known has E_a, the activation energy which can be obtained from Arrhenius Eq. (11):

$$k = Ae^{-\frac{E_a}{RT}} \quad (11)$$

Where k is reaction rate, A is pre-exponential factor, E_a is the activation energy, R is the gas constant, and T is the temperature usually measure in kelvin.

On logarithmic expression, Eq. (11) become Eq. (12):

$$\ln k = -\frac{E_a}{RT} + \ln A \quad (12)$$

The graph of ln k is plotted against 1/T, the slope (m) of the graph estimated stand for $\left(-\frac{E_a}{R}\right)$, and the activation energy Ea was obtained using Eq. (13):

$$E_a = -m(R) \quad (13)$$

2.7. Determination of thermodynamic parameter of transesterification reaction

Based on biodiesel conversion, the correlating equation that involves two liquids utilization can be expressed by equation of Eyring Polanyi (Eqn. 14), which relate the entropy (ΔS^{θ}) and enthalpy (ΔH^{θ}), both are the thermodynamic parameter for biodiesel conversion.

$$\frac{k}{T} = \frac{kK_B}{h} . e^{\frac{\Delta S^{\theta}}{R}} . e^{-\frac{\Delta H^{\theta}}{RT}} \quad (14)$$

On logarithmic expression, Eq. (14) become Eq. (15):

$$\ln\left(\frac{k}{T}\right) = ln\left(\frac{K_B}{h}\right) + \frac{\Delta S^{\theta}}{R} - \frac{\Delta H^{\theta}}{RT} \quad (15)$$

Where K_B is the Boltzmann's Entropy Constant (1.360649×10^{-23} J/K), h is the Planck's constant ($6.62607015 \times 10^{-34}$ m^2kg/s).

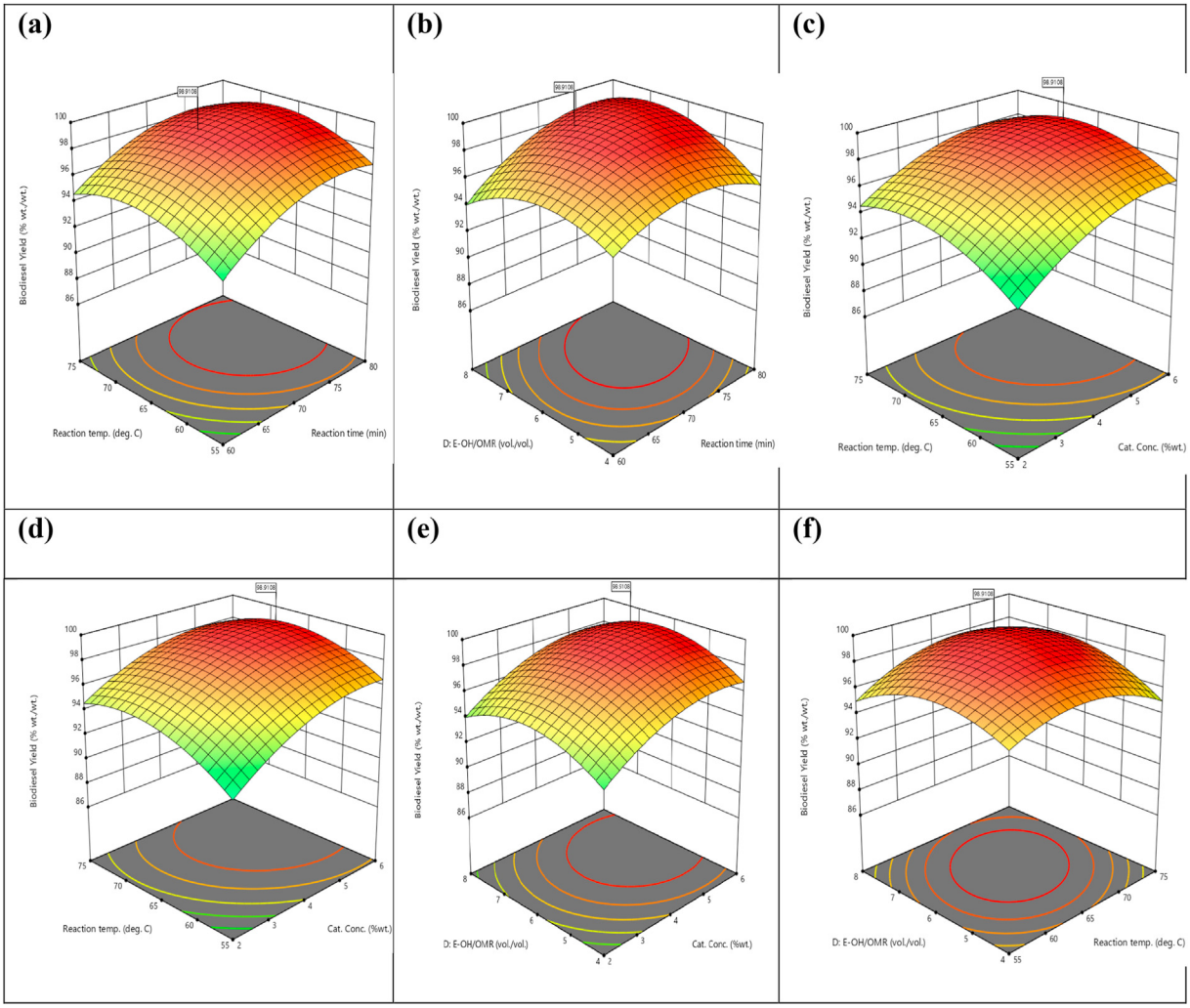

Figure 7. The contour and three dimensional plots.

Therefore, based on the molar quantity of the binary mixture from measurement of composition dependence of the corresponding total molar quantity, Gibb's-Duhem equation was applied as written in Eq. (16):

$$\Delta G^{\theta} = \Delta H^{\theta} - T\Delta S^{\theta} \tag{16}$$

2.8. Catalyst reusability test

Catalyst recoverability was carried out after reaction completion through filtration. Prior to re-usability test, the recovered catalyst was cleaned by washing with alcohol to remove the adhered impurities, centrifuge for 600 min at 4000 rpm, and then filtered to separate the supernatant from the residual catalyst. The residual catalyst was oven dried to constant weight and then cools at room temperature for 50 min before reused. Each experiment for catalyst reusability test was carried out in duplicate and the mean average was used at the maximum biodiesel yield and variable constraint conditions. A total of 10 cycled runs were performed and the yields were recorded.

3. Results and discussion

3.1. Properties of EGO, TRO, and mixed oil (MO)

Displayed in Table 2 are the physicochemical properties of the oils extracted from the seeds. The properties of the oil were taking in the mean average, and the mixed oil ratio of 2:3 was obtained by calculating the API gravity of the oil total. The properties of the mixed oil was also evaluated which showed that the mixed oil (MO) has low free fatty acid (0.98); therefore it required a single stage transesterification process. The high cetane (59.84) and higher heating value (39.70) of the mixed oil indicated that the oil has tendency to produce carrier energy. Nevertheless, the high density (900.20 kg/m^3) of the mixed oil indicated that the transesterification of the oil will reduced the oil density to required value via transesterification reaction.

3.2. Analysis of developed catalyst the CLLSP

3.2.1. BET analysis of CLLSP

Presented in Figure 1 is the BET adsorption analysis of the calcined catalyst sample (CLLSP) with the help of data acquisition method engaged with N_2 adsorbate for sample weight of 1.2×10^{-4} kg. Revealed in the figure is the graph of pore volume against diameter with optimum volume and diameter of 0.318 (cc/g) and 2.80 nm, respectively. The inverse relationship exists between the diameter and pore volume along with the synthesis of biodiesel. Meanwhile, Figure 2 showed the two dimensional plots of cumulative pore volumes and pore diameter. High catalytic reactivity was noticed at low pore volume of 0.217 cc/g, high surface area of 442.718 m^2/g, and high pore diameter of 2.432 nm. Further analysis results are displayed in supplementary file.

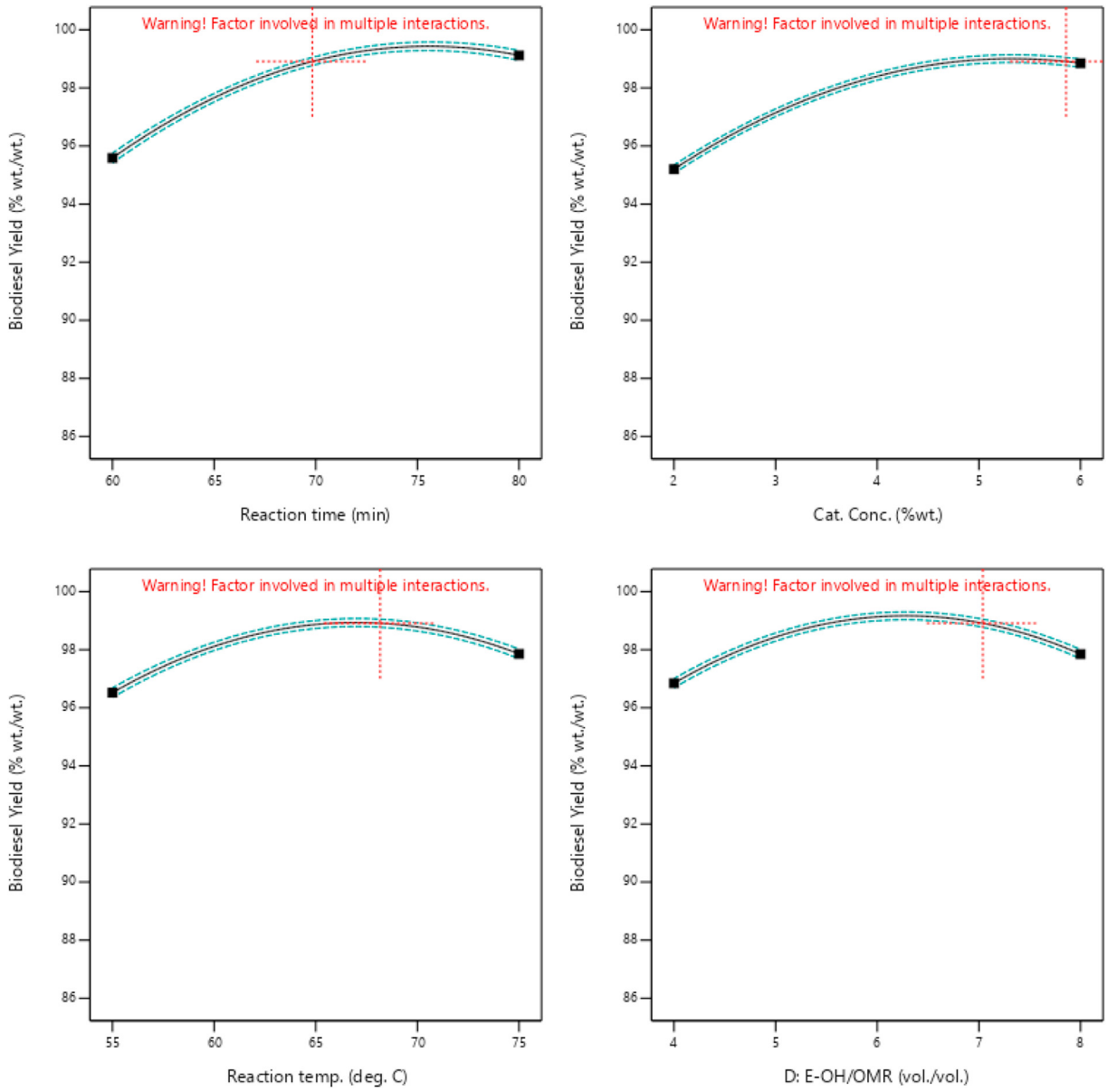

Figure 8. Factors effects of variables on the response.

3.2.2. XRS-FP analysis

Table 3 presented the results obtained from XRS-FP analysis through Gaussian method. The analysis resulted in elemental evolution with calcium oxide (CaO = 89.457 (wt. %)) as dominant compound. The presence of other compound such as silica (SiO_2 = 3.555 (wt. %)), alumina (Al_2O_3 = 3.950 (wt. %), and ferric oxide (Fe_2O_3 = 1.704 (wt.%)). The high CaO indicated the complete decomposition of catalyst during calcination which connoted the presence of base catalyst used for biodiesel production. The presence of Al_2O_3 observed in the catalyst indicated another base support compound for high CaO found. The identification of SiO_2 in the sample proved that catalyst is acidic in nature, but also act as weak base.

3.3.3. SEM analysis

The structural SEM images of the calcined sample are displayed in Figure 3, performed at magnification of 500x and 1000x. The image structure showed a muddy crystal-like cohesive outlook. The structure also showed shining jointed attribute with aggregate of most pores gathered together, exhibited bod structures. The soapy look could be attributed to the presence of SiO_2 found in the catalyst. However, the whiteness, brightness and opacity look could be due to SnO_2 found in the sample. The brilliant glossy glaze, whitish appearance, caustic alkaline, and crystalline solid at room temperature could be attributed to the presence of CaO and Al_2O_3, which make CLLSP good candidates for the synthesis of biodiesel.

3.2.4. FTIR analysis

Displayed in Figure 4 is the FTIR analysis result of the CLLSP showing the images of wavelength against the transmittance at various phase angles. Observation proved that numerous compounds noticed at the peak of calcined sample. The found peak at 648.1 showed the occurrence of a well aliphatic compound and - C_nH_{2n} with shaking elasticity. The established peaks between 1256.35 and 1635.69 reflected the involvement of existence of hexane in cyclo ring ambiances, methane C–H bond, C–H symmetry of methyl, the twist C–C vinyl bend, olefinic of C=C alkenyl expanse, aryl substituted C=C, and conjugate C=C. The functional groups observed from 129.48 to 2885.6 indicated the presence of methyl C–H asymmetry and symmetry stretch, also present is methylene C–H stretch. Further peaks noticed from 3356.25 to 3927.2 represent the region of single bond, Hydroxyl group, H-bonded OH stretch, Phenols, OH stretch, Alcohol (primary, secondary,

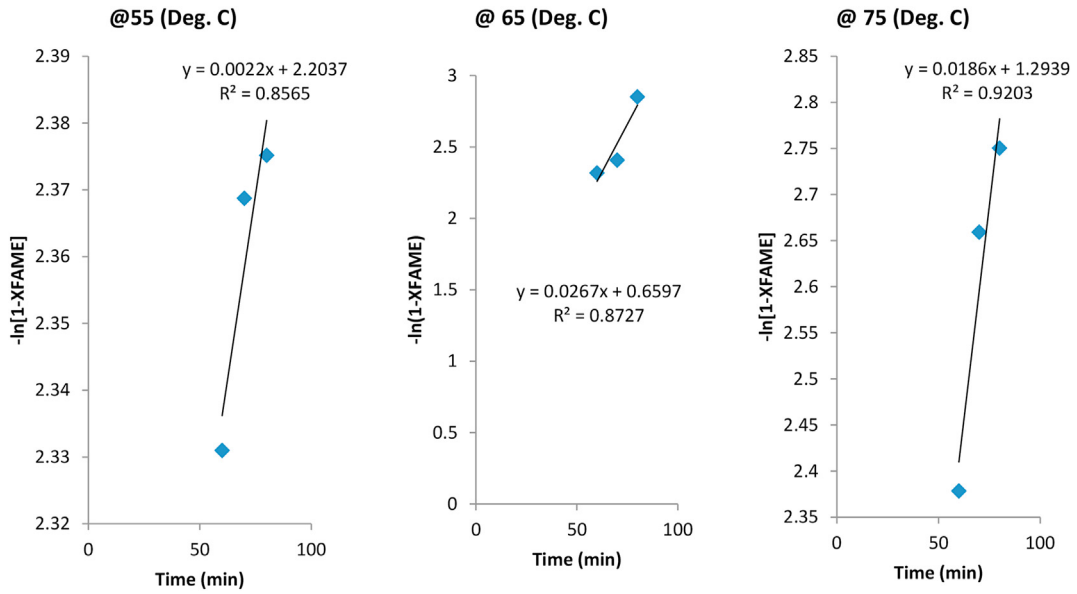

Figure 9. Plot of $-ln|1-X_{FAME}|$ vs. time interval (t).

Table 6. Values of Rate constant (k) and R.^{2}.

Temperature (^{o}C)	Temperature (K)	R^2	k (min^{-1})
55	238	0.8565	0.0022
65	248	0.8727	0.0267
75	258	0.9203	0.0186

and tertiary), Ca–O bonding, and Dimeric OH stretch. The high peak of 3927.2 obtained proved that the liberation of CaO from $CaCO_3$ was completed during calcination. The peak values, the intensity, the base H, base L, area and corr. Area are present in Supplementary file.

3.2.5. *Effects of thermal decomposition of powdery catalyst for biodiesel*

Thermal heat treatment contributes significantly to the FAME (biodiesel) conversion. The calcined catalyst and non calcined catalyst were tested for biodiesel production. The conversion of FAME was not found when un-calcined catalyst was used. This indicated that, the activity of catalyst need to be integrated based on surface area with the aids of heat treatment. At temperature of 100 °C to 500 °C, the FAME conversion rate started forming, but the yield was 20% (wt./wt). An increased in calcination temperature between 550 °C to 1000 °C produced high conversion of FAME but much higher at 850 °C. This showed that at 550 °C to 850 °C, the conversion of $CaCO_3$ to CaO start degradation with complete evolution of CO_2 and only remains of CaO at 750 °C to 850 °C (Figure 5). This is observed in increased FAME conversion from 20 to 100% as the thermal temperature increased from 550 °C to 850 °C. However, FAME conversion reduces when the thermal temperatures get to 900 °C and 1000 °C which may be due to aggregation and cluster attributes of the calcined catalyst. Therefore, the calcined temperature that produced high FAME conversion is the optimum calcined temperature for catalytic conversion of the powder to catalyst response for FAME conversion of ≈99% (wt.).

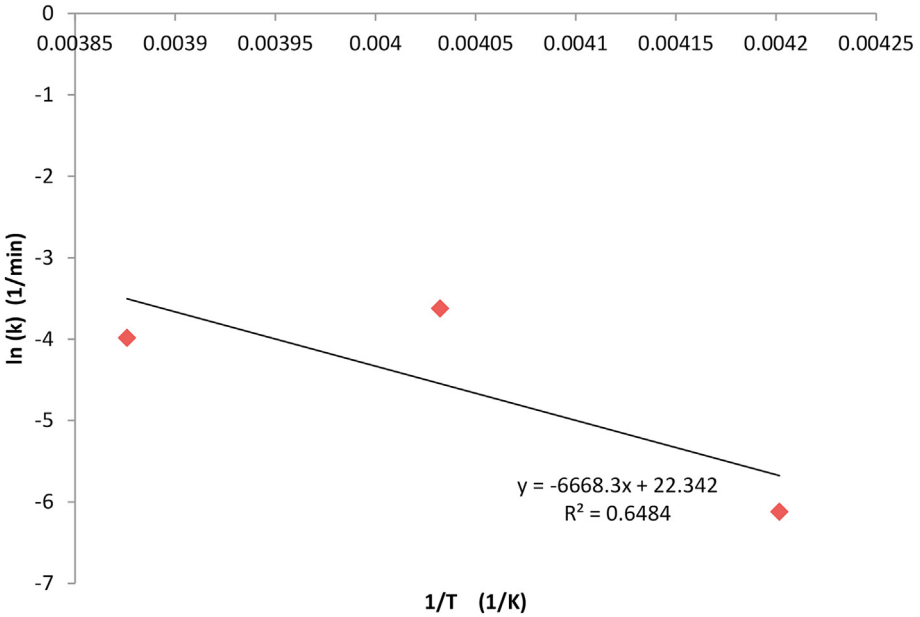

Figure 10. Plot of ln (k) against 1/T.

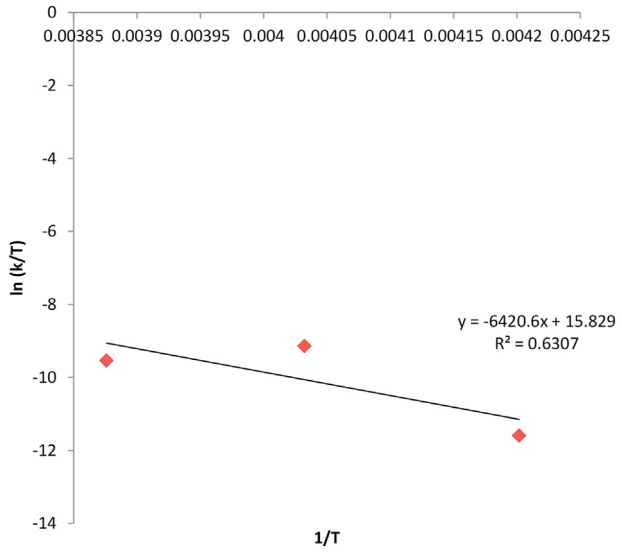

Figure 11. The plot of $ln(\frac{k}{T})$ vs. $\frac{1}{T}$

3.4. Modeling and optimization of transesterification reaction

Table 4 showed the results of average mean of experimental biodiesel yield carried out in duplication with predicted value by the CCD and the residual value, all within the thirty experimental runs generated with constraint variables. From the result, the highest biodiesel yield was 98.60 (% wt./wt) at Runs 6, 20, 26, and 28, while the lowest yield was Run 6. These values were subject to analysis the predicted value gave way for the error term as the difference between the experimental yield and the predicted. To show the relationship between the.

experimental and predicted yield, a plot in Figure 6(a) was used, which showed a perfect straight line via the origin, while the graph of normal probability against external studentized residual with intercept was displayed in Figure 6(b). Further analysis via test of ANOVA, Fits, statistical test, and a quadratic model test, which produced remarkably significant results with P-values all$<$ 0.05, with high F-values indicated significant model terms (Table 5). The results observed for fit statistical test indicated a high percentage of regression parameter in terms of coefficient of.

determination with R^2 = 99.89%, Adj. R^2 = 99.79%, and Pred. R^2 = 99.39. The Predicted R^2 of 99.39% is in reasonable agreement with the Adjusted R^2 of 99.79; i.e. the difference is less than 0.5. However, based on model quadratic, the model equation that established the relationship between the linear, quadratic, and the interactions of variables and the response (biodiesel) is given by Eq. (17) in coded value form.

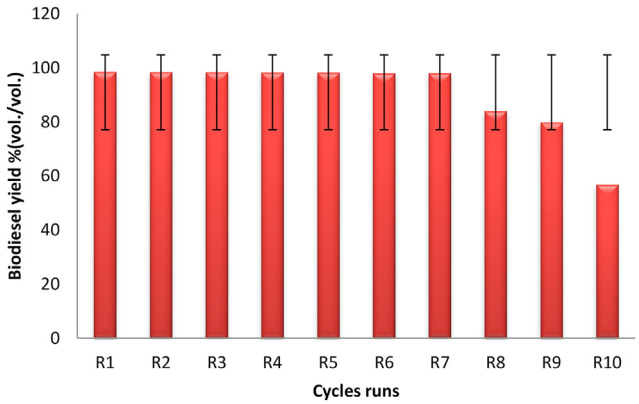

Figure 12. Catalyst reusability test plots.

Table 7. Summary table of thermodynamics properties of biodiesel synthesis.

Thermodynamics properties	Temperature (K)		
	238	248	258
ΔG^{θ}	174.67 kJ mol^{-1}	179.77 kJ mol^{-1}	184.87 kJ mol^{-1}
ΔH^{θ}	53.38 kJ mol^{-1}		
ΔS^{θ}	-509.64 J mol^{-1}		

$$\text{Biodiesel yield}(\%\ wt/wt) = 98.67 + 1.01X_1 + 1.88X_2 + 0.5962X_3 + 0.1921X_4 + 0.3031X_1X_2 - 0.1094X_1X_3 + 0.9894X_1X_4 - 0.3306X_2X_3 + 0.10312X_2X_4 + 0.7281X_3X_4 - 1.59X_1^2 - 1.37X_2^2 - 1.68X_3^2 - 1.78X_4^2 \quad (17)$$

To determine the optimum biodiesel yield under different variables condition, the CCD was set to optimization techniques and the results was confirmed graphically. The numerical examination predicted the optimum biodiesel yield of 98.91% (wt./wt.) at the following variable conditions: X_1 = 69.83 (min), X_2 = 5.86 (%wt.), X_3 = 68.17 °C, and X_4 = 7.04 (vol./vo.). To confirmed the optimum yield, the result was validated in five (5) experimental runs at the same conditions, and the average mean value was obtained as 98.90% (wt./wt.). The graphical displayed of interaction among the variables on response are illustrated in Figure 7(a-f)., as the contour and three dimensional plots, while the effect of each factor on the response are displayed in Figure 8 which confirmed the optimum condition for biodiesel yield.

3.5. Kinetic of transesterification study

The kinetic study of transesterification reaction was carried out based on pseudo first order reaction employing percentage biodiesel conversion (FAME) and reaction time. From Eq. (11), $-ln|1 - X_{FAME}|$ vs. time interval (t) (Figure 9) was plotted at various temperature of 55, 65, and 75 °C, and at catalyst concentration of 2, 4, and 6 (% wt.) with E-OH/OMR of 4:1, 6:1, and 8:1 based on validated optimum condition level.

From the plots, the coefficient of determination R^2 can be obtained, the slopes of the graph can be used to evaluate the values of rate constant k (min^{-1}). These results are presented in Table 6 as the value of temperature, the coefficient of determination R^2, and the slope of the graph as rate constant k.

Further analysis involved the plot of ln (k) against 1/T (Figure 10) to obtained the slope (-E_a/R) as indicated in Eq. (13), and the value of activation energy E_a was calculated using Eq. (14)

The minimum amount of energy that was provided for the transesterification reaction to produced biodiesel otherwise known as activation energy of the transesterification was determined to be 55.44 kJ mol^{-1} (taking R = 8.3145 J. mol^{-1}. K^{-1}) with R^2 of 64.84%. The value

Table 8. Properties of biodiesel.

Parameter	Biodiesel	ASTM D6751	EN 14214
Colour@ 27 °C	Yellow brownish	-	-
Density (kg/m^3) @ 25 °C	860	-	860–900
Viscosity @ 40 °C/(mm^2/s)	1.20	1.9–6.0	3.5–5.0
Moisture content (%)	0.01	$<$0.03	0.02
%FFA (as oleic acid)	0.12	0.40 max	0.25 max
Acid value (mg KOH/g oil)	0.24	0.80 max	0.5 max
Iodine value (g I_2/100g oil)	65.10	-	120 max
Saponification value (mg KOH/g oil)	125.20	-	-
Peroxide value (meq O_2/kg oil)	5.60	-	12.85
HHV (MJ/kg)	43.32	-	-
Cetane number	75.25	57 min	51 min
API	32.93	39.95 max	-

reported in this work is far better than the values reported by other previous researchers [38, 39, 40].

3.6. Thermodynamics parameter of transesterification study

Based on thermodynamic study of the transesterification reaction, Eyring Polanyi equation was implemented (Eqn. 16), the plot of $ln\left(\frac{k}{T}\right)$ vs. $\frac{1}{T}$ was carried out with slope $\left(\frac{-\Delta H^{\theta}}{R}\right)$. From Figure 11, the slope of the graph (−6420.6) gave a ΔH^{θ} of 53.38 kJ mol^{-1} which is the enthalpy of reaction. This simply means that the amount of energy gained during transesterification reaction is high enough to produced energy fuel.

The thermodynamic properties also known as entropy ΔS^{θ} was evaluated based on Eyring Polanyi equation with relationship with the intercept (15.829) was -509.64 J mol^{-1} ("-" means decreased in transesterification reaction disorder). The ΔG^{θ} at different reaction temperatures of the transesterification reaction can be estimated from Gibb's Duhem Eq. (17), and the results are presented in Table 6. The table showed that the highest amount of energy obtained during transesterification process was at higher temperature which helps the spontaneous reaction of the reaction, making it a continuous processing.

3.7. Catalyst reusability test

One of the key advantages of heterogeneous catalyst over the homogeneous catalyst is the ability to be recycled and reused. In this study, the strength of the derived base catalyst was confirmed using recyclability test. The recycled catalyst was tested in a total of ten (10) experimental runs and the yields of the biodiesel were potted against the number of cycle runs. Figure 12, Showed the results obtained using excel plot with error bars. It was observed that the biodiesel yield was not significantly affected by the number of cycle runs up to seven cycles, but their exist a great decreased in the amount of biodiesel form eight to tenth runs. Hence, catalyst recyclability was altered at seventh runs. The deceased in the catalyst active basic strength may be attributed to reduction in surface area as results of impurities adhered to the surface of catalyst, and the formation of calcium-glyceroxide [11, 41].

3.8. Quality of biodiesel

The qualities of biodiesel produced were examined by determining the physicochemical properties using AOAC, 1997 methods, and the results were compared with biodiesel recommended standard. Presented in Table 7 are the results of the properties of biodiesel produced. The results indicated that the observed biodiesel qualities were in line with the standard laid down by American and European standard for biodiesel [42, 43]. This implies that the produced biodiesel in this work can replace conventional diesel use in industries and for commercial purposes (see Table 8).

4. Conclusion

In this study, biodiesel was synthesized from the mixture of two oils using the blend ratio of 2:3 based on API gravity of the oil. Catalytic analysis indicated CaO as the major elemental composition of the derived base catalyst with 89.46%. Process optimization thru CCD produced a validated optimum biodiesel yield of 98.90% (wt./wt.) at the following optimized conditions: $X_1 = 69.83$ (min), $X_2 = 5.86$ (%wt.), $X_3 = 68.17$ °C, and $X_4 = 7.04$ (vol./vo.). The regression parameter evaluation produce a coefficient of determination with $R^2 = 99.89\%$, Adj. $R^2 = 99.79\%$, and Pred. $R^2 = 99.39$. The kinetic study revealed the transesterification process produced activation energy of the 55.44 kJ mol^{-1} with R^2 of 64.84%. The thermodynamics of the reaction indicated a high Gibbs free energy of reaction. Catalyst reusability test was altered at 7th runs owing to low biodiesel yield. The qualities of the produced biodiesel were in line with the standard laid down by American and European standard for biodiesel [42,43].

Declarations

Author contribution statement

Eyibio, U. P: conceived and designed the experiments; wrote the paper.

Ukanwa, K. S: conceived and designed the experiments; performed the experiments; analyzed and interpreted the data.

Amabogba, E, Adebayo, A. D: performed the experiments; analyzed and interpreted the data.

Adepoju, T. F: analyzed and interpreted the data; wrote the paper.

Balogun, T. A, Eloka-eboka, A. C: contributed reagents, materials, analysis tools or data.

Funding statement

This research did not receive any specific grant from funding agencies in the public, commercial, or not-for-profit sectors.

Data availability statement

Data included in article/supp. material/referenced in article.

Declaration of interest's statement

The authors declare no conflict of interest.

Additional information

No additional information is available for this paper.

Acknowledgements

In carrying out the Catalyst characterization and analysis, the efforts of technical staff of Spectral Laboratory Services of Engineering and Science Analyses, No. 14 Forte Oil Station, Kaduna, Nigeria are highly appreciated. During the laboratory and in gathering the waste materials, the supports of project students 2020/2021 of Engr. Dr. Adepoju T. F. are highly appreciated.

References

[1] https://www.eiu.com/n/energy-in-2022-transition-time/retrieved, 2022.
[2] https://www.theworldcounts.com/retrieved, 2022.
[3] R. Kukana, O.P. Jakhar, Synthesis of biodiesel from prosopis juliflora and using MCDM analytical hierarchy process technique for evaluating with different biodiesel, Cogent Eng. 8 (2021), 1957291.
[4] E.A. Olatundun, O.O. Borokini, E. Betiku, Cocoa pod husk-plantain peel blend as a novel green heterogeneous catalyst for renewable and sustainable honne oil biodiesel synthesis: a case of biowastes-to-wealth, Renew. Energy 166 (2020) 163–175.
[5] O. Sahu, Characterisation and utilization of heterogeneous catalyst from waste rice-straw for biodiesel conversion, Fuel 287 (2020), 119543.
[6] M. Balaji, S. Niju, Banana peduncle–A green and renewable heterogeneous base catalyst for biodiesel production from Ceiba pentandra oil, Renew. Energy 146 (2020) 2255–2269.
[7] O.E. Anietie, P. Musonge, A.C. Eloka-eboka, Evaluation of in-situ and ex-situ hybridization in the optimized transesterification of waste and pure vegetable oils, Biofuel Bioprod. Bioref. (2022).
[8] T.F. Adepoju, Y.T. Hung, Optimization processes of biodiesel production from pig and neem (*Azadirachta indica* A. Juss) seeds blend oil using alternative catalysts from waste biomass, in: L.K. Wang, M.H.S. Wang, Y.T. Hung (Eds.), Waste Treatment in the Biotechnology, Agricultural and Food Industries, Handbook of Environmental Engineering, 26, Springer, Cham, 2022.
[9] T.F. Adepoju, H.A. Akens, B.E. Ekeinde, Synthesis of Biodiesel from Blend of Seeds Oil-Animal Fat Employing Agricultural Wastes as Base Catalyst, CSCEE, 2022a.
[10] M. Balajii, S. Niju, Banana peduncle–A green and renewable heterogeneous base catalyst for biodiesel production from Ceiba pentandra oil, Renew. Energy 146 (2020) 2255–2269.
[11] T.F. Adepoju, U.P. Eyibuo, R.E. Emberru, T.A. Balogun, Optimization Conversion of Beef Tallow Blend with Waste Used Vegetable Oil for Fatty Acid Ethyl Ester (FAEE) Synthesis in the Presence of Bio-Base Derived from *Theobroma Cacao* Pod Husks, CSCEE, 2022b.

[12] I.M. Nurudeen, A.K. Nassereldeen, A. Md Zahangir, E.S. Mohamed, A. Mirghani, Optimization of *jatropha* biodiesel production by response surface methodology, Green Sustain. Chem. 11 (2021) 23–37. https://www.scirp.org/journal/gsc.

[13] E.O. Ajala, M.A. Ajala, A.O. Ajao, H.B. Saka, A.C. Oladipo, Calcium-carbide residue: a precursor for the synthesis of $CaO–Al_2O_3–SiO_2–CaSO_4$ solid acid catalyst for biodiesel production using waste lard, Chem. Eng. J. Adv. 4 (2020), 100033.

[14] R. Rajendran, B. Kanimozhi, P. Prabhavathi, K.S. Dinesh, P. Santhanam, M. Abirami, S.S. Karthik, A. Manikandan, A method of central composite design (CCD) for the optimization of biodiesel production from Chilorella vulgaris, J. Petrol Environ. Biotechnol. 6 (2015) 3.

[15] M. Moslen, C.H. Adiela, Consumption Safety in Relation to Bioaccumulation of Heavy Metals in Perinwinkles (Tympanotonus Fuscatus) Obtained from Ogbia in the Niger Delta Region of Nigeria, 2020.

[16] C. Okoye, O. Chinenye, I. Nwokedi, O.C. Eije, E.I. Asimobi, Biodiesel synthesis from waste cooking oil using periwinkle shells as catalyst, J. Energy Res. Rev. (2020).

[17] A. Ataei-Azimi, B.D. Hashemloian, H. Ebrahimzadeh, A. Majd, High in Vitro Production of Ant-Canceric Indole Alkaloids from Periwinkle (Catharanthus Roseus) Tissue culture, Afr. J. Biotechnol. 7 (16) (2008) 1684–5315, eiSSN.

[18] I. Thushari, S. Babel, Biodiesel production from waste palm oil using palm empty fruit bunch-derived novel acid catalyst, J. Energy Res. Technol. Trans. ASME 140 (3) (2017).

[19] M. Mujtaba, M. Kalam, H. Masjuki, M.E.M. Soudagar, H.M. Khan, H. Fayaz, M. Farooq, M. Gul, W. Ahmed, M. Ahmad, Effect of palm-sesame biodiesel fuels with alcoholic and nanoparticle additives on tribological characteristics of lubricating oil by four ball tribo-tester, Alex. Eng. J. 60 (2021) 4537–4546, 2021.

[20] S. Sahani, Y.C. Sharma, Economically viable production of biodiesel using a novel heterogeneous catalyst: kinetic and thermodynamic investigations, Energy Convers. Manag. 171 (2018) 969–983.

[21] AOAC, Official Methods of Analyses of the Association of Official Analytical Chemists, 1997.

[22] Standard Test Method for Gross Calorific Value of Oil, Water, Coal and Coke by the adiabatic Bomb Calorimeter from SAI Global. ASTM D2051

[23] S.K. Haldar, B.B. Ghosh, A. Nag, Utilization of unattended *Putranjiva roxburghii* non-edible oil as fuel in diesel engine, J. Renew. Energy 34 (2009) 343–347.

[24] T.F. Adepoju, V.I. Etim, R.I. Uzono, T.A. Balogun, E.R. Emberru, An application of Non-edible oils, Bio-base catalyst, and Process optimization as an economical route for a hybridized oil biodiesel synthesis, Case Stud. Chem. Environ. Eng. 6 (2022c), 100231, 2022.

[25] T.F. Adepoju, M.A. Ibeh, A.J. Asuquo, Elucidate three novel catalysts synthesized from Animal bones for the production of biodiesel from ternary non-edible and edible oil blend. A case of *Jatropha curcus, Hevea brasiliensis, and Elaeis guineensis* oils, S. Afr. J. Chem. Eng. (2021a).

[26] A.D. Tadesse, T.M. Tadios, S.M. Yedilfan, Optimized biodiesel production from waste cooking oil (WCO) using calcium oxide (CaO) nano-catalyst, Sci. Rep. 9 (2019), 18982.

[27] H.M. Khan, T. Iqbal, S. Yasin, C.H. Ali, M.A. Mujtaba, M.A. Jamil, A. Hussain, M.E.M. Soudagar, M.M. Rahman, Application of agricultural waste as heterogeneous catalysts for biodiesel production, Catalysts 11 (2021) 1215, 2021.

[28] T.F. Adepoju, H.A. Akens, B.E. Ekeinde, Synthesis of biodiesel from blend of seeds oil-animal fat employing agricultural wastes as base catalyst, Case Stud. Chem. Environ. Eng. (2022d).

[29] Eriola Betiku, Tunde F. Adepoju, Akinbiyi K. Omole, Seyi E. Aluko, Statistical approach to the optimization of oil from beniseed *(Sesamum indicum)* oilseeds, J. Food Sci. Eng. 2 (2) (2012) 351–357. https://www.academia.edu/23782490.

[30] H. Hadiyanto, P.L. Sri, W. Widayat, Preparation and characterization of *anadara granosa* shells and $CaCO_3$ as heterogeneous catalyst for biodiesel production, Bull. Chem. React. Eng. Catal. 11 (2016) 21–26.

[31] N. Subramaniapillai, V. Govindaraj, B. Muthusamy, Process optimization of *Calophyllum inophyllum*-waste cooking oil mixture for biodiesel production using Donax deltoids shells as heterogeneous catalyst, Sustain. Environ. Res. 29 (2019) 2351–2362.

[32] O. Okwundu, A. El-Shazly, M. Elkady, Comparative effect of reaction time on biodiesel production from low fatty acid beef tallow: a definition of production yield, SN Appl. Sci. 1 (2019) 140.

[33] J. Gupta, M. Agarwal, Preparation and characterizaton of CaO nanoparticle for Biodiesel production, AIP Conf. Proc. (2016).

[34] V.B. Veljković, A.V. Veličković, J.M. Avramović, O.S. Stamenković, Modeling of biodiesel production: performance comparison of box–Behnken, face central composite or full factorial design, Chin. J. Chem. Eng. (2018) (in press).

[35] G.R. Moradi, M. Mohadesi, M. Ghanbari, M.J. Moradi, S. Hosseini, Y. Davoodbeygi, Kinetic comparison of two basic heterogenous catalysts obtained from sustainable resources for transesterification of waste cooking oil, Biofuel Res. J. 6 (2015) 236–241.

[36] E.A. Olatundun, O.O. Borokini, E. Betiku, Cocoa pod husk-plantain peel blend as a novel green heterogeneous catalyst for renewable and sustainable honne oil biodiesel synthesis: a case of biowastes-to-wealth, Renew. Energy 166 (2020) 163–175.

[37] T.F. Adepoju, E.N. Udoetuk, B.E. Olatunbosun, I.A. Mayen, R. Babalola, Evaluation of the effectiveness of the optimization procedure with methanolysis of waste oil as case study, S. Afr. J. Chem. Eng. 25 (2018) 169, 17.

[38] K. Cholapandian, B. Gurunathan, N. Rajendran, Investigation of CaO nanocatalyst synthesized from Acalypha indica leaves and its application in biodiesel production using waste cooking oil, Fuel 312 (2022), 122958.

[39] S. Sahani, Y.C. Sharma, Economically viable production of biodiesel using a novel heterogeneous catalyst: kinetic and thermodynamic investigations, Energy Convers. Manag. 171 (2018) 969–983.

[40] A. Sharma, P. Kodgire, S.S. Kachhwaha, Investigation of ultrasound-assisted KOH and CaO catalyzed transesterification for biodiesel production from waste cotton-seed cooking oil: process optimization and conversion rate evaluation, J. Clean. Prod. 259 (2020), 120982.

[41] H.H. Abdelhady, H.A. Elazab, E.M. Ewais, M. Saber, M.S. El-Deab, Efficient catalytic production of biodiesel using nano-sized sugar beet agro-industrial waste, Fuel (2020) 261.

[42] Standard Test Method for Gross Calorific Value of Oil, Water, Coal and Coke by the adiabatic Bomb Calorimeter from SAI Global. ASTM D6751

[43] European Committee for Standardization, describing the requirements and test methods for FAME. EN 14214.